NUMERICAL STUDY OF TURBULENT HEAT TRANSFER IN A TRAPEZOÏDAL CHANNEL WITH FLAT BAFFLES

Younes Menni*, Ahmed Azzi, Chafika Zidani
Research Unit of Materials and Renewable Energies (URMER),
Department of Physics, Faculty of Sciences, Abou Bekr Belkaid University,
BP 119-13000-Tlemcen, Republic of Algeria, Tel./Fax: +213 43215890/89
*Corresponding author. E-mail: menniyounes.cfd@gmail.com
Reçu le: 10/02/2016 Accepté le: 19/06/2016

Abstract
This paper presents flow configurations and heat transfer characteristics in an isothermal trapezoidal channel with staggered flat baffles. The fluid is considered, Newtonian, incompressible with constant properties. The CFD software FLUENT 6.3 is used to simulate the fluid flow and heat transfer fields. The governing equations, based on the SST k-ω model used to describe the turbulence, are discretized using the finite volume approach. The numerical results were compared with available experimental data from the literature and good agreement is obtained.
Keywords: *CFD - Finite volume method - Flat baffle - Trapezoidal channel.*

Résumé
Dans le présent travail les caractéristiques d'écoulement et de transfert thermique dans une conduite de section trapézoïdale munie de chicanes rectangulaires disposées en chevauchement est mise en étude. Le fluide est considéré, Newtonien, incompressible à des propriétés constantes. Les équations gouvernantes, basées sur le modèle k-ω SST, sont résolues par la méthode des volumes finis. Le logiciel de calculs numériques en dynamique des fluides FLUENT 6.3 a été appliqué pour intégrer ces équations sur chaque volume de contrôle. Les résultats obtenus sont très concordants aux résultats numériques et expérimentaux de la littérature.
Mots-clés: *CFD - Méthode des volumes finis - Chicane plane - Conduite trapézoïdale.*

1. INTRODUCTION

The most commonly used technique for internal cooling enhancement is the placement of baffles and fins. These deflectors are generally mounted on the heat transfer surface, which disturbs the boundary layer growth and enhances the heat exchange time between fluid and the heated surfaces. Several studies have been undertaken, in this context, in order to optimize their size [1], their position [2], their arrangement [3], their orientation [4] and their shape [5-8].

2. PHYSICAL MODEL

This numerical contribution investigates the momentum and heat transfer characteristics and the associated frictional head loss in a trapezoidal-channel with staggered vertical solid baffle plates. A combination of two flat-baffles of same overall size is used in this simulation. A schematic view of the physical problem is shown in Figure 1. Dimensions are based on the experimental study of Demartini et al. [5]. Air is selected as the working fluid.

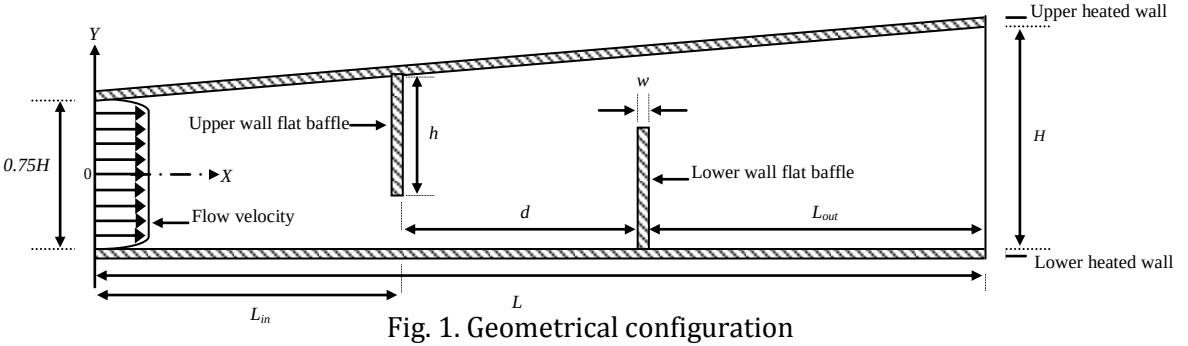

Fig. 1. Geometrical configuration

3. MATHEMATICAL MODELLING

The numerical fluid flow and heat transfer in the trapezoidal channel is developed under the following assumptions: (1) Steady two-dimensional flow and heat transfer, (2) The flow is turbulent and incompressible, (3) Constant fluid properties, (4) Body forces, viscous dissipation and radiation heat transfer are ignored.

Based on the above assumptions, the channel flow model is governed by the Reynolds averaged Navier-Stokes (RANS) equations with the SST k-ω model and the energy equation. All the equations are discretized by the QUICK scheme and SIMPLE algorithm is implemented. The detail on mathematical modeling can be found in the work published by Menni et al. [9]. Five parameters of interest in the present work are the Reynolds number (Eq. 1), friction coefficient (Eq. 2), friction factor (Eq. 3), local (Eq. 4) and average (Eq. 5) Nusselt numbers, details of which can be found in Menni et al. [10].

To validate the numerical model, the axial velocity profile obtained from the current CFD simulation was compared with the one

obtained from the experimental work of Demartini et al. [5] for the airflow flow inside a two-dimensional rectangular channel with upper and lower wall-mounted baffle plates at Re = 8.73×10^4 as shown in Figure 2. For x = 0.525m and as can be seen, there is a good consistency between the experimental and numerical data which indicates that the numerical calculation method is valid.

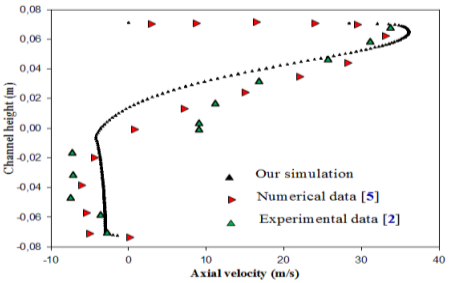

Figure 2. Comparison of the experimental and numerical results.

4. RESULTS AND DISCUSSION

The flow characteristics in the trapezoidal-channel with two flat-baffles placed in opposite walls in a periodically staggered way are presented in terms of fields and profiles of axial velocities as shown in Figures 3-7.

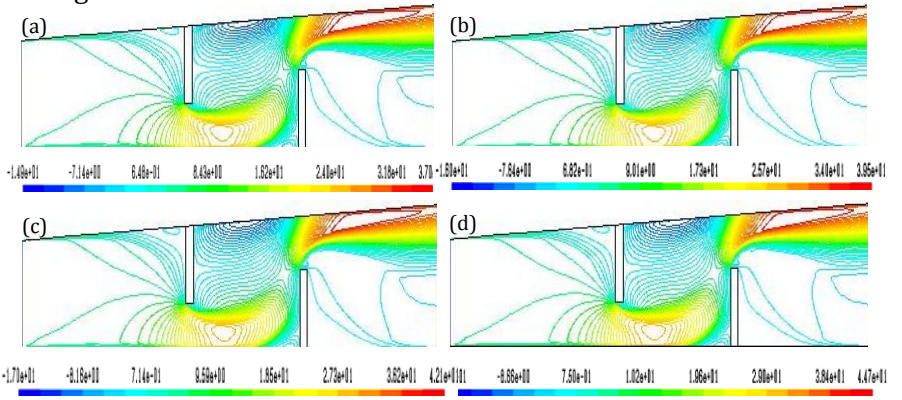

Fig. 3. Variation plots of axial velocity fields with Reynolds number: (a) Re = 8.73×10^4, (b) Re = 9.33×10^4, (c) Re = 9.93×10^4, and (d) Re = 10.53×10^4.

Figure 3a-d displays the contour plots of axial velocity fields on the longitudinal section with lower and upper wall-mounted rectangular-baffles at different Reynolds number values (Re). In the figure, the plots show very low velocity values adjacent to the flat-baffles. In the regions downstream of both baffle plates, recirculation cells with very low velocity values are observed. In the regions between the tip of the baffles and the channel walls, the velocity is increased. Due to the changes in the flow direction produced by the considered baffles, the highest velocity values appear near the upper channel wall with an acceleration process that starts just after the second baffle. This behavior is very similar to the distribution observed in tube banks with baffle plates (Demartini et al. [5]) with higher velocity values. The effects of the flow rate in terms of Reynolds number with four Re values (Re = 8.73×10^4, 9.33×10^4, 9.93×10^4, and 10.53×10^4) for using the flat-baffles on the flow field in the form of axial velocity are also depicted in Figure 3a-d, respectively. In the figure, it is interesting to note that the axial velocity value tends to increase with the rise of Reynolds number values for all areas. The velocity value at Re = 9.33×10^4, 9.93×10^4, and 10.53×10^4 is found to be around 5.064, 5.397, and 5.732 times higher than that with Re = 8.73×10^4, respectively. Figure 4a and b shows the axial velocity distribution upstream of the first baffle on the sections x = 0.159m and x = 0.189m, measured downstream of the entrance, respectively.

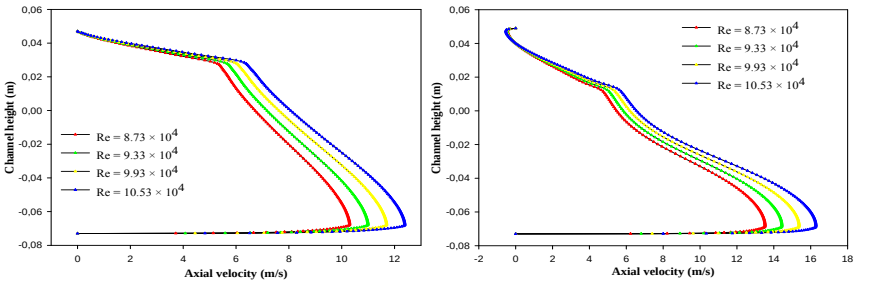

Fig. 4. Variation of axial velocity profiles with Re upstream of the first baffle at (a) x = 0.159 m, and (b) x = 0.189m from the entrance.

It can be seen that the influence of the deformation of the flow field increases as the flow approaches the first flat-baffle, increasing the velocity of the flow approaching the passage under the flat-baffle,

in accordance with the results by Demartini et al. [5]. The graphical representations of the axial velocity profiles variation as a function of Reynolds number in different sections of the channel, at locations given by x = 0.255m and x = 0.285m from entrance, respectively 0.027 and 0.057 m after the first flat-baffle, are shown in Figure 5a and b, respectively. In the figure, a strong clockwise vortex is observed downstream of the first flat-baffle, which was induced due to the flow separation. This recirculation zone is located close to the solid wall in the upper part of the channel and its height is approximately equal to the extent of the flow blockage by the baffle plates, which is equal to 0.08m. This corresponds to the area reduction of 54% at the baffle edge.

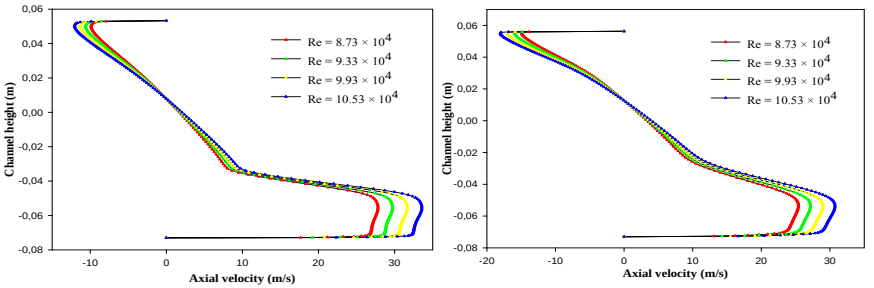

(a) (b)

Fig. 5. Variation of axial velocity profiles with Re behind the first baffle at (a) x = 0.255 m, and (b) x = 0.285 m from the entrance.

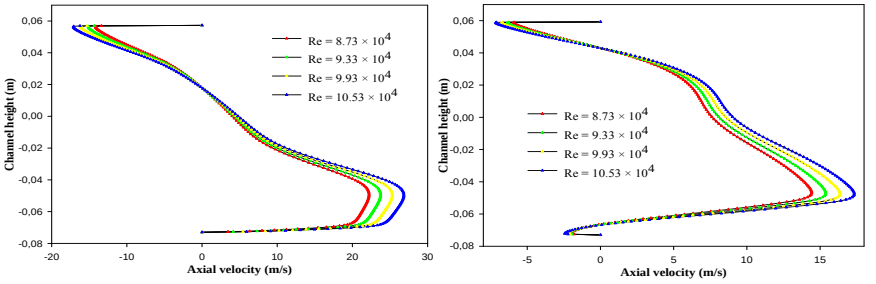

(a) (b)

Fig. 6. Variation of axial velocity profiles with Re between the first and second baffles at (a) x = 0.315 m, and (b) x = 0.345 m from the entrance.

These observations showed the same behavior as Nasiruddin and Kamran Siddiqui [4] results. In the regions between the tip of the considered baffle plate and the lower channel wall, the velocity is

increased, approaching 352.526 - 430.457 % of the reference velocity, which is 7.80 m/s, depending on the Reynolds number values. The comparison of axial velocity profile distributions at different Reynolds numbers for positions x = 0.315m (see Fig. 6a) and x = 0.345m (see Fig. 6b), respectively 0.055m and 0.025m before the lower flat- baffle, shows that as the flow is accelerated and redirected near the second baffle plate, a very small counterclockwise vortex with very low velocity values is formed in the vicinity of the lower left corner, while in the upper part the flow starts to accelerate toward the gap above the lower wall flat-baffle, as shown in Figure 6. In the upper part of the channel, near the top heated wall, the negative velocities indicate the presence of the clockwise recirculation behind the first flat-baffle. These results showed the sam et al. [2] results except for flow a

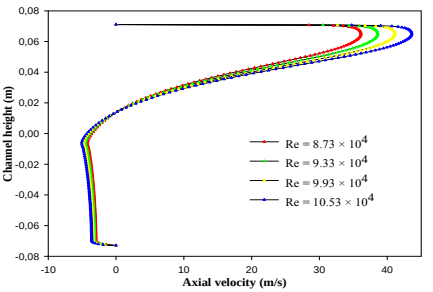

Fig. 7. Variation of axial velocity profiles with Re after the lower wall baffle, near the channel outlet at x = 0.525 m.

In the region downstream of the second flat baffle, near the channel outlet, at axial location x = 0.525m from entrance, 0.029 mm before the channel exit, as a result of sudden expansion in the cross-section, the flow separates, a larger counterclockwise vortex is formed behind the lower wall obstacle and flow reattachment is then established as indicated by Mohammadi Pirouz et al. [2] (See Fig. 7). The highest velocity values are found in the region opposite the second flat-baffle, near the upper channel wall, due to the changes in the flow direction produced by both baffle plates.

The flow velocity is also affected by the Reynolds number (see Figs. 3-7). The results show that the air flow is accelerating in its main direction from left towards right-hand side (positive direction) by

increasing the recirculation zones size hence the length of these regions of recycling is proportional to the increase in the flow rate. This result can be explained by the fact of the input velocity increase of air flow and also the convective heat transfer from the surfaces of the channel walls to the following air.

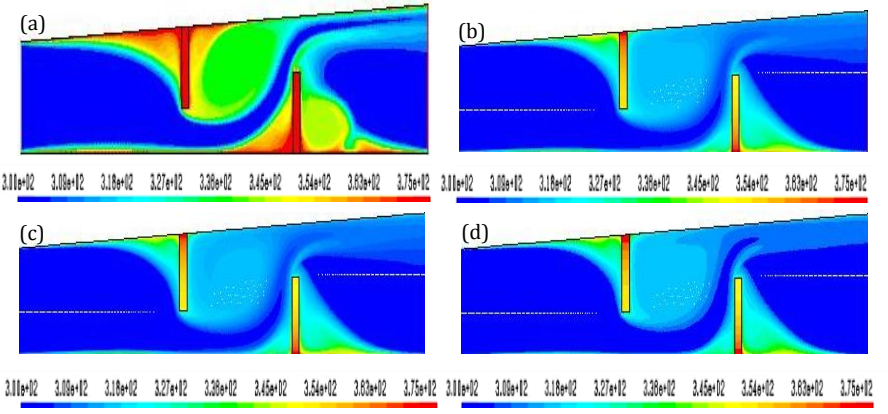

Fig. 8. Variation of temperature fields with Re: (a) Re = 8.73×10^4, (b) Re = 9.33×10^4, (c) Re = 9.93×10^4, and (d) Re = 10.53×10^4.

Figure 8 presents the contour plots of temperature field distributions for air flow in the trapezoidal-channel with two staggered rectangular-baffles in the case of different Reynolds number values (Re = 8.73×10^4, 9.33×10^4, 9.93×10^4, and 10.53×10^4). The plot shows that the fluid temperature in the recirculation region is significantly high as compared to that in the same region of no baffle case, in accordance with the results reported by Nasiruddin and Kamran Siddiqui [4]. The results show that there is a major change in the temperature field along both channel heated walls, especially in the region opposite the flat-baffle tip. This means that the recirculation zone provide a significant influence on the temperature field, because they can induce better fluid mixing between the wall and the core regions, leading to a high temperature gradient along the heating channel wall, as indicated by Sripattanapipat and Promvonge [6]. Concerning the effect of the Reynolds number on the isotherms, it can see from this figure that the higher of Re results in the rise of flow rate, causing the better mixing of the fluid flow and intensity of the vortex strength. The heat transfer coefficient is presented in this section in terms of local

and average Nusselt numbers as shown in Figures 9 and 10, respectively. In Figure 9, the local Nusselt number is related as a function of Reynolds number along the heated top channel wall. The Nu_x values tend to drop considerably to almost zero when it reaches and passes the first flat-baffle.

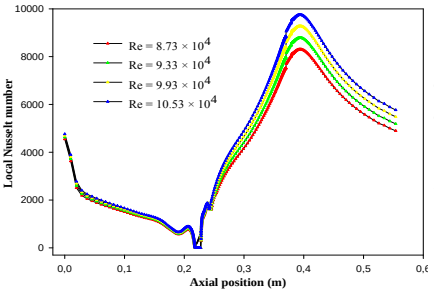

Fig. 9. Variation of Nu_x with Re along the top heated channel wall.

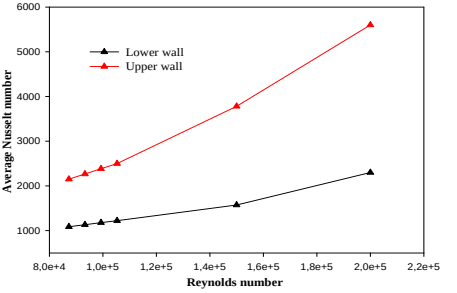

Fig. 10. Average Nusselt number versus Re.

The figure shows that in the region downstream of the upper wall baffle, located at a distance of x = 0.218m from the entrance, the local Nusselt number is enhanced. This enhancement is due to the intense mixing by the clockwise vortex. These results are confirmed by Nasiruddin and Kamran Siddiqui [4] results. The placement of the upper wall flat-baffle at the beginning of the heated channel disturbs the boundary layer formation and contributes to higher heat transfer as indicated by Dutta and Hossain [3]. In addition, the plot shows that the maximum Nu_x occurs in the region opposite the lower wall flat-baffle due to the high velocities in that region. In the figure, the characterization plot also shows that the Nu_x increases with an increase in the Re value. This could be due to the reason that an increase in the Re causes an increase in the length of the recirculation zone, which enhances mixing and mixing length. The influence of Re on the evolution of the average Nusselt number, Nu_{av} is presented in Figure 10 where it is shown an increase of the heat transfer rate by increasing Reynolds number due to the augmentation of the inertia forces further to the augmentation of the flow rate. The largest variations are found on the top channel wall, due to the strong velocity gradients in that region.

The profile plots of local skin friction coefficient, *Cf* along the upper wall of the channel are shown in Figure 11 for different Reynolds number values. In these plots, the *Cf* is increased again at the locations corresponding to the zones of clockwise vortex as seen behind the first flat-baffle.

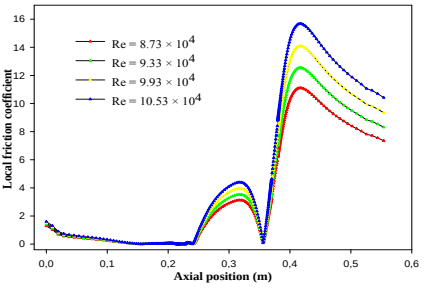

Fig. 11. Variation of C*f* with Re along the upper heated wall.

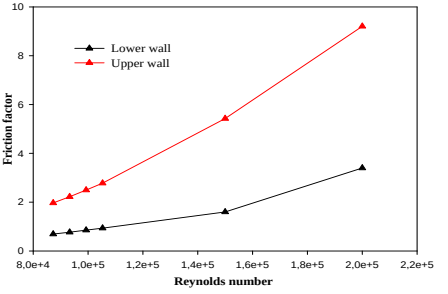

Fig. 12. Friction factor versus Re.

It indicates that the highest *Cf* can be observed at the area of high velocity in the region opposite of the second flat-baffle especially near the tip of the lower wall flat-baffle due to the changes in the flow direction produced by the baffle plates while the lowest of the *Cf* is found in the region upstream of the upper wall flat-baffle for all locations caused by the absence of the obstacles. The *Cf* is also affected by the Reynolds number (see Fig. 11). As expected, the skin friction shows the same trend as the local Nusselt number, shown in Figure 9. The pressure loss in terms of friction factor along the top and bottom heated surfaces of the trapezoidal-channel for the same geometry is presented in figure 12 for the same range of Reynolds numbers. At Reynolds numbers of 8.73×10^4 - 10.53×10^4, the figure shows that the friction loss tends to increase with the rise of Re values for both the top and bottom heated walls of the channel. Thus the flow blockage due to the existence of baffle as well as the role of turbulence degree in the core region is a key factor to cause an extreme pressure drop as reported by Sripattanapipat and Promvonge [6]. Similarly to the results in Figure 10, the upper friction loss values at the heated top channel surface are due to the high velocities in that region.

5. CONCLUSION

In this article, the turbulent heat transfer and friction loss distribution study in a constant temperature-surfaced trapezoidal section channel with upper and lower wall-mounted baffles has been investigated by CFD method. The largest variations in Nusselt number and skin friction are found near the tips of the flat-baffles, due to the strong velocity gradients in that region, and in general, an increase in the Re cause a substantial increase in the velocity and heat transfer but the friction loss is also very significant.

References

[1] P. Dutta, S. Dutta, Effect of baffle size, perforation and orientation on internal heat transfer enhancement, Int. J. Heat Mass Transfer 41(19) (1998) 3005-3013.
[2] M. Mohammadi Pirouz, M. Farhadi, K. Sedighi, H. Nemati, E. Fattahi, Lattice Boltzmann simulation of conjugate heat transfer in a rectangular channel with wall-mounted obstacles, Scientia Iranica B 18 (2) (2011) 213-221.
[3]P. Dutta a, A. Hossain, Internal cooling augmentation in rectangular channel using two inclined baffles, Int. J. Heat and Fluid Flow 26 (2005) 223-232.
[4] Nasiruddin, M.H. Kamran Siddiqui, Heat transfer augmentation in a heat exchanger tube using a baffle, Int. J. Heat and Fluid Flow 28 (2006) 318-328.
[5] L.C. Demartini, H.A. Vielmo, S.V. Möller, Numeric and experimental analysis of the turbulent flow through a channel with baffle plates J. the Braz. Soc. of Mech. Sci. & Eng. 26(2) (2004) 153-159.
[6] S. Sripattanapipat, P. Promvonge, Numerical analysis of laminar heat transfer in a channel with diamond-shaped baffles, Int. Commun. Heat Mass Transfer 36 (2009) 32-38
[7] W. Jedsadaratanachai, N. Jayranaiwachira, P. Promvonge, 3D numerical study on flow structure and heat transfer in a circular tube with V-baffles, Chinese Journal of Chemical Eng. 23 (2015) 342-349.
[8] P. Sriromreun, C. Thianpong, P. Promvonge, Experimental and numerical study on heat transfer enhancement in a channel with Z-shaped baffles, Int. Commun. Heat Mass Transfer 39 (2012) 945-952.
[9] Y. Menni, A. Azzi, C. Zidani, Computational analysis of turbulent forced convection in a channel with staggered corrugated baffles, COST N° 16 (2016).
[10] Y. Menni, A. Azzi, C. Zidani, Etude numérique comparative entre deux types de chicanes et ailettes (rectangulaire et rectangulaire

arrondie) utilisées pour améliorer les performances des capteurs solaires plans à air, Revue des Energies Renouvelables 18(3) (2015) 347-361.